Measurement of x-ray emission from Gd, Dy, and Er stimulated by 59.54-keV photons

C. Baraldi,[1,2,3,*] E. Casnati,[1,2,3] A. Tartari,[1,2,3] G. Di Domenico,[1,3] and B. Singh[1,†]

[1]*Dipartimento di Fisica, Università di Ferrara, I-44100 Ferrara, Italy*
[2]*Istituto Nazionale di Fisica della Materia, Unità di Ferrara, I-44100 Ferrara, Italy*
[3]*Istituto Nazionale di Fisica Nucleare, Sezione di Ferrara, I-44100 Ferrara, Italy*

(Received 19 July 1999; published 16 February 2000)

Accurate measurements, within 2%, of *K* radiation emission cross sections were carried out on thick foils of ^{64}Gd, ^{66}Dy, and ^{68}Er stimulated by 59.54-keV photons, i.e., an energy close to the *K* thresholds of the target atoms. The results obtained provide a good global reference test for the relativistic quantum-mechanic models used in the calculations of *K* fluorescence yields and *K* vacancy creation cross sections.

PACS number(s): 32.80.Fb

INTRODUCTION

Accurate measurements of the $\omega_K\tau_K$ cross section of *K* photoelectric emission, that is the *K* x-ray fluorescence (XRF) cross section, are useful in order to check the reliability of calculation models used in the evaluation of fundamental atomic parameters such as *K* fluorescence yield and *K*-shell vacancy creation cross section. These data are even more important just above the *K* threshold of the elements.

A complete theoretical model of atom readjustment after a vacancy creation in its *K* shell was worked out by Chen, Crasemann, and Mark [1], who combined *K*-shell Auger rates calculated by the DHS (Dirac-Hartree-Slater) atomic model with the DF (Dirac-Fock) radiative rates given by Scofield [2]. Their data concern 25 elements in the range $18 \leqslant Z \leqslant 96$. Recently, Perkins *et al.* [3] presented an ω_K tabulation for all the most common *Z* values. They combined DHS Auger rates, calculated from the library of the Lawrence Livermore Laboratory, with the DHS radiative rates of Scofield [4]. Bambynek *et al.* [5] and Krause [6] evaluated *K* fluorescence yields by interpolating experimental and theoretical data with a semiempirical formula, while Hubbell [7] gave ω_K values obtained using the same formula but with the coefficients proposed by Bambynek [8]. More recently, Hubbell *et al.* [9] presented an ω_K tabulation obtained by interpolating all the experimental values collected over the period 1978–1993 on 55 elements with *Z* in the interval 11–93.

Exhaustive reviews on photoelectric effect cross sections were prepared by Pratt, Ron, and Tseng [10], Cooper [11], Hubbell and Veigele [12], and Starace [13]. For energies greater than 1 keV and $1 \leqslant Z \leqslant 101$ the main theoretical compilations of self-consistent data are all based on the electron-independent atomic model, and are due to Storm and Israel [14], Plechaty, Cullen, and Howerton [15], and Scofield [16]. The latter compilation includes values of relativistic photoelectric cross sections of the whole atom and of each atomic shell calculated by the DHS atomic model, using theoretical energy levels; the conversion factors of each shell from DHS to DHF (Dirac-Hartree-Fock) for $Z \leqslant 54$ are also given. Scofield's is the most detailed theoretical compilation; his values are taken as a reference by more elaborate theoretical methodologies [17], and are used as database for the evaluation of photoelectric attenuation coefficients [18] and for photon transport codes [19]. Chantler [20] recently prepared a tabulation of the photoelectric attenuation coefficients of the atom as a whole and of the *K* shell alone using the DHF atomic model, but with Kohn-Sham exchange potential and experimental energy levels. However, the most rigorous and accurate procedure for calculating the photoelectric cross section is the one based on the QED approach restricted to the second-order *S* matrix in the independent-particle approximation. This procedure was successfully applied by Kissel, Pratt, and Roy [17] and Kissel *et al.* [21] to compute the elastic scattering amplitudes. Unfortunately, a tabulation of photoelectric cross sections based on this methodology has not yet been prepared owing to the very long computing time required.

Experimental evaluations of *K*-shell radiation emission with uncertainties comparable to those of the different theoretical calculations can be of great help in checking the reliability of the products $\omega_K\tau_K$ calculated by the theoretical and interpolated values of *K* fluorescence yield, and by the *K* photoelectric cross section obtained by different quantum-mechanical models. These comparisons are still more interesting for targets with *K* electron binding energies just below that of impinging photons because, in this region, the photoelectric cross section is a rapidly varying function of the ratio between incident photon and target *K* threshold energies. The present paper gives the results of measurements of fluorescence *K* radiation emitted by foils of elements with $64 \leqslant Z \leqslant 68$ stimulated by photons of 59.54 keV, i.e., an energy close to that of the target *K* thresholds.

Measurements of *K* photoelectric emission that include ^{64}Gd, ^{66}Dy, and ^{68}Er were carried out with 59.54-keV photons by Balakrishna *et al.* [22] and Ertuğrul *et al.* [23]. The first group of researchers measured the *K* emission of 29 $\leqslant Z \leqslant 92$ target foils by a HPGe detector and ^{241}Am and ^{203}Hg sources in reflection geometry. From their measurements they derived and presented the ω_k values of 16 elements. The second group measured the K_α radiative emis-

*Electronic address: baraldi@fe.infn.it

†Permanent address: Physics Department, Punjabi University, Patiala, India.

sion of elements in the range $64 \leqslant Z \leqslant 68$ by a Si(Li) detector and a ^{241}Am source in transmission geometry. Both groups used thin targets.

MEASUREMENT METHODOLOGY

As the geometrical arrangement and experimental methodology have been described in previous papers [24,25], just the points that favor an understanding of the present results are recalled here. The experiment was carried out in specular geometry with source-to-target and target-to-detector distances approximately equal to one another, and very great with respect to the target thicknesses. Both the source (18.5 GBq of ^{241}Am) and the detector (high-purity Ge 200 mm^2 in area and 10 mm in thickness) were equipped with multivane collimators to reduce the divergence of the primary beam and the acceptance angle of the detector. This arrangement ensured irradiation uniformity, because the target surface seen by the detector was smaller than the target-irradiated area. With this experimental arrangement it is possible to show that the detector counting rate is given by

$$N_\delta = An\sigma_j' \frac{1-\exp[-(\mu_i+\mu_\delta)L/\cos\gamma]}{\mu_i+\mu_\delta}\varepsilon_\delta \exp(-\mu_{a\delta}L_a). \tag{1}$$

In this expression, μ_i is the linear attenuation coefficient of the radiation impinging the target foil of thickness L, and σ_j' the differential cross section of the interaction process j between photon and atom giving rise to the emission of δ-type photons with linear attenuation coefficient μ_δ in the target material. L_a is the air thickness between target and detector, $\mu_{a\delta}$ the attenuation coefficient of δ-type photons in air, and ε_δ the physical efficiency of the detector. A is a coefficient depending on the incident flux density and geometrical factors of the experiment, and n is the atom volume density of the irradiated target.

By placing

$$\mathcal{A}_\delta = \frac{1-\exp[-(\mu_i+\mu_\delta)L/\cos\gamma]}{\mu_i+\mu_\delta}, \quad \mathcal{B}_\delta = \epsilon_\delta \exp[-\mu_{a\delta}L_a],$$

expression (1) can be written as

$$N_\delta = An\sigma_j' \mathcal{A}_\delta \mathcal{B}_\delta. \tag{2}$$

When the interaction process is the creation of a vacancy in the K level, an α or β x-ray photon is emitted. The energies within each α or β group are usually so close that only one attenuation coefficient need be considered for all the photons of a group. Let p_α and p_β denote the fractions of the radiative transitions of K vacancies giving rise to photons of α and β type, respectively, and with $\mathcal{A}_K\mathcal{B}_K$ the quantity

$$\mathcal{A}_K\mathcal{B}_K = p_\alpha \mathcal{A}_\alpha \mathcal{B}_\alpha + p_\beta \mathcal{A}_\beta \mathcal{B}_\beta.$$

So if the cross section of the K radiation isotropically emitted by the target of atomic number Z is $\sigma_K' = \omega_K \tau_K$, the counting rate per unit solid angle of both α and β x-rays is given by

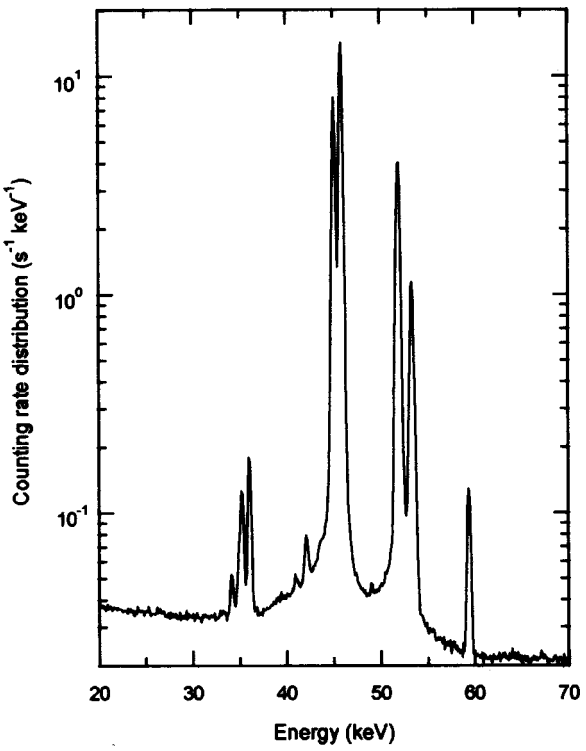

FIG. 1. Example of a distribution in energy of Dy foil count rates measured under an angle of 90° with the incident beam axis.

$$N_K = An_Z \frac{\omega_K \tau_K}{4\pi} \mathcal{A}_K \mathcal{B}_K.$$

The incident photon energy is close to the K threshold energies of the target elements, and therefore, in the measured spectrum shown in Fig. 1, the elastic peak is not far from the photoelectric α and β K peaks. Moreover, owing to the relatively low primary photon energy, the incoherent scattered contribution may partially overlap both the K peaks, and the HPGe detector gives a K_β escape falling in the range of the K_α peak. All these drawbacks make the correct evaluation of the K counting rate rather complicated. For incoherent scattering events with differential cross section σ_I', expression (2) becomes

$$N_I = An_Z \sigma_I' \mathcal{A}_I \mathcal{B}_I$$

while for elastic scattering with differential cross section σ_E', the analogous expression is

$$N_E = An_Z \sigma_E' \mathcal{A}_E \mathcal{B}_E.$$

The coefficient A can be removed by normalizing the total counting rate $N_T = N_K + N_I + N_E$ measured by the target of interest to the counting rate N_{Be} of the incoherent radiation scattered by a ^{4}Be target. Using σ_{Be}' to indicate the ^{4}Be incoherent scattering cross section, the counting rate due to this radiation is

$$N_{\mathrm{Be}} = An\sigma_{\mathrm{Be}}' \mathcal{A}_{\mathrm{Be}} \mathcal{B}_{\mathrm{Be}}$$

TABLE I. Properties of the target foils. E_K, K threshold energy [26]; E_i/E_K, incident photon energy normalized to the threshold one; P purity, $\mathcal{L}=\rho L$, mass thickness; $s_{\mathcal{L}}$, standard deviation of $\mathcal{L}$ over the irradiated area; $(f_\alpha)_{\pi/4}$, $(f_\beta)_{\pi/4}$, $(f_C)_{\pi/4}$, $\pi/4$ saturation factors for K_α, K_β, and Compton-scattered radiation.

Element	Z	E_K (keV)	E_i/E_K	P %	$\mathcal{L}$ (mg/cm^2)	$s_{\mathcal{L}}$ (mg/cm^2)	$(f_\alpha)_{\pi/4}$	$(f_\beta)_{\pi/4}$	$(f_C)_{\pi/4}$
Be	4	0.1117		99.8	103.30	0.26			0.0427
Gd	64	50.239	1.185	99.9	82.82	0.10	0.870	0.842	
Dy	66	53.788	1.107	99.9	112.58	0.11	0.942	0.925	
Er	68	57.486	1.036	99.9	96.42	0.40	0.919	0.901	

and the cross section $\omega_K\tau_K$ of K radiation emission can be written as

$$\omega_K\tau_K=\frac{4\pi}{\mathcal{A}_K\mathcal{B}_K}\left\{\frac{N_T}{N_{\mathrm{Be}}}\sigma'_{\mathrm{Be}}\mathcal{A}_{\mathrm{Be}}\mathcal{B}_{\mathrm{Be}}\frac{\rho_{\mathrm{Be}}M_Z}{\rho_Z M_{\mathrm{Be}}}-\sigma'_I\mathcal{A}_I\mathcal{B}_I-\sigma'_E\mathcal{A}_E\mathcal{B}_E\right\}, \tag{3}$$

where M_Z,ρ_Z and $M_{\mathrm{Be}},\rho_{\mathrm{Be}}$ are the atomic mass and the density of the element of interest and ^{4}Be, respectively.

Table I gives the properties of the examined target foils and the $\pi/4$ saturation factor defined as

$$(f_\delta)_{\pi/4}=1-\exp[-(\mu_i+\mu_\delta)L\sqrt{2}]$$

for their α and β characteristic K radiation and for the incoherent radiation scattered once by ^{4}Be. Apart from the ^{4}Be foil, the targets examined have saturation factors close to 1. This choice greatly improves the signal-to-noise ratio [27], because the reduction in the statistical uncertainty due to larger countings exceeds the increase caused by the uncertainty of the factor correcting the signal enhancements for double and higher-order scatterings.

Three independent measurements were carried out on each target at each of the three angles 60°, 90°, and 120°. Targets and angles were alternated so as to check measurement reproducibility and to randomize geometry uncertainty.

The ^{4}Be data processing followed the same procedure as that previously described [24].

To obtain K counts the whole spectral distribution, as given in Fig. 1, was considered. After background subtraction, its area from about 3 keV below the lowest energy K_α escape peak to 1 keV above the elastic scattering peak was evaluated. With such a choice no K escape correction was needed because these peaks, together with the once-scattered continuum, are totally included in the estimate. Great attention was devoted to the enhancements in K and elastic peaks and in incoherent distribution owing to double and multiple interactions. The enhancement factors were calculated in two ways: by the expressions given by Casnati *et al.* [28] and by a photon transport Monte Carlo program. To this end, the EGS4 code modified by Namito, Ban, and Hirayama [29] to include the Doppler-broadening of Compton-scattered photons was used. This code was still further improved by adding the effect of anomalous dispersion on photon elastic scattering; the effect is important in the region of the threshold energy and the area of the elastic peak was appreciably changed. The enhancement factors obtained by the two procedures for all the experimental conditions and interactions examined differed in any case by less than 1%. Therefore, in the calculations the rapidity of the analytical expression was preferred and, for its values, a rectangular distribution with 1% maximum uncertainty was assumed [30].

The value of p_α and p_β were obtained from Scofield's ratios $R=p_\beta/p_\alpha$ [31], to which a stochastic uncertainty of 1% was assigned, bearing in mind the comments of Khan and Karimi [32]. The attenuation coefficients required by the expressions of $\mathcal{A}_\alpha$, $\mathcal{A}_\beta$, $\mathcal{A}_I$, $\mathcal{A}_E$, $\mathcal{B}_\alpha$, $\mathcal{B}_\beta$, $\mathcal{B}_I$, $\mathcal{B}_E$, $\mathcal{A}_{\mathrm{Be}}$, and $\mathcal{B}_{\mathrm{Be}}$ were calculated by averaging the values of the compilations of Veigele [33], Plechaty, Cullen, and Howerton [15], and Storm and Israel [14], and of Scofield's [16] tabulation combined with that of Hubbell *et al.* [34]. The σ'_I differential cross sections were derived from the calculations of Hubbell *et al.* [34], while the σ'_E differential elastic cross sections were taken from Kissel and Bergstrom [35].

To obtain the standard deviation of the K emission cross section, the uncertainties of all the quantities appearing in expression (3) were combined in quadrature by excluding those with relative values below 10^{-5}.

TABLE II. Theoretical and interpolated values of K fluorescence yield. $(\omega_K)_P$, Perkins *et al.* [3]; $(\omega_K)_B$, Bambynek *et al.* [5]; $(\omega_K)_K$, Krause [6]; $(\omega_K)_{H1}$, Hubbell [7]; $(\omega_K)_{H2}$, Hubbell *et al.* [9].

Element	Z	$(\omega_K)_P$	$(\omega_K)_B$	$(\omega_K)_K$	$(\omega_K)_{H1}$	$(\omega_K)_{H2}$
Gd	64	0.935	0.934	0.935	0.932	
Dy	66	0.940	0.940	0.941	0.938	0.972
Er	68	0.944	0.945	0.947	0.942	

TABLE III. Theoretical values of vacancy creation in K shell by 59.54-keV photons. $(\tau_K)_S$, Scofield by including nuclear size effects [16, 36]; $(\tau_K)_C$, Chantler [20]; $(\tau_K)_K$, Kissel [37].

Element	Z	$(\tau_K)_S$ (barn)	$(\tau_K)_C$ (barn)	$(\tau_K)_K$ (barn)
Gd	64	2490	2493	2490
Dy	66	2750	2753	2754
Er	68	3016	3018	3018

TABLE IV. Comparison of K photoelectric emission cross sections. $(\omega_K\tau_K)_{PS}$, ω_K by Perkins *et al.* [3]; τ_K by Scofield [16, 36]; $(\omega_K\tau_K)_{H2S}$, ω_K by Hubbell *et al.* [9]; τ_K by Scofield [16, 36]; $(\omega_K\tau_K)_F$, present experiment values; $(\omega_K\tau_K)_B$, values derived from the experiment of Balakrishna *et al.* [22]; $(\omega_K\tau_K)_E$, values derived from the experiment of Ertuğrul *et al.* [23].

Element	Z	$(\omega_K\tau_K)_{PS}$ (barn)	$(\omega_K\tau_K)_{H2S}$ (barn)	$(\omega_K\tau_K)_F$ (barn)	$(\omega_K\tau_K)_B$ (barn)	$(\omega_K\tau_K)_E$ (barn)
Gd	64	2327		2319 ± 30	2270 ± 112	2299 ± 155
Dy	66	2585	2673	2591 ± 47	2623 ± 132	2554 ± 135
Er	68	2842		2800 ± 50		2825 ± 175

EXPERIMENTAL RESULTS AND DISCUSSION

Theories give separate values of the ω_K fluorescence yield and of the K creation vacancy cross section τ_K, while experiments provide only the product $\omega_K\tau_K$. Therefore, comparisons between experiment and theory require theoretical data for both these quantities.

Theoretical and interpolated semiempirical values of K fluorescence yield are collected in Table II. The first column lists the examined elements and the second their atomic number. The third column gives the theoretical values calculated by Perkins *et al.* [3] by combining DHS nonradiative transitions with the radiative ones obtained by Scofield using the DHS model [4]. Another theoretical tabulation was prepared by Chen, Crasemann, and Mark [1], who combine their Auger rates with the DF radiative ones by Scofield [2]. Unfortunately these data do not include ^{64}Gd, ^{66}Dy, and ^{68}Er, but the mean difference between the values of Chen, Crasemann, and Mark and those of Perkins *et al.* is barely 0.2% in the $63\leqslant Z\leqslant 70$ interval; thus different theoretical treatments give ω_K values that do not differ appreciably in the Z range of interest. Consequently, the ^{64}Ge, ^{66}Dy, and ^{68}Er ω_K theoretical values directly calculated by Perkins *et al.* [3] are the ones used in the present comparison. The interpolated semiempirical data of Bambynek *et al.* [5], Krause [6], Hubbell [7], and Hubbell *et al.* [9] are also collected in columns 4, 5, 6, and 7 of Table II. As may be seen, the values of the first three sets do not greatly differ from each other or from the theoretical one, while the only value of Hubbell *et al.* [9] reported in the table is a little greater.

Tabulations of the photoelectric cross section that include only the whole atom τ_a data are unsuitable, because accurate τ_K cannot be obtained by the simple relation

$$\tau_K=\tau_a\frac{r_K-1}{r_K}.$$

In fact, as Pratt, Ron, and Tseng [10] pointed out—and as the tabulations of Scofield [16] and Chantler [20] show—the r_K jump changes with photon energy. Theoretical values of τ_K for 59.54-keV photons have been calculated by Scofield [16,36] and Chantler [20] using central potential models with different approximations, and by Kissel [37] with the second-order perturbative S matrix. As can be seen in Table III, the differences between the sets of values are not significant.

In this context, Perkins *et al.* ω_K fluorescence yields combined with the τ_K values of Scofield's thorough tabulation on K vacancy creation cross sections were used to calculate theoretical $(\omega_K\tau_K)_T$ K radiation emission cross sections.

Experimental data similar to the present data still require some adjustment in order to permit an acceptable comparison. Balakrishna *et al.* [22] multiplied their measured $\omega_K\tau_K$ K emission cross sections by τ_K to present ω_K fluorescence yield values. The τ_K were evaluated using an interpolation procedure described by the authors. The same procedure applied backward provides $(\omega_K\tau_K)_B$ K emission cross sections from the ω_K presented. Ertuğrul *et al.* [23] measured K_α emission cross sections; therefore, by multiplying their $\omega_K\tau_{K\alpha}$ values by $1+p_\beta/p_\alpha$, one derives $(\omega_K\tau_K)_E$ cross sections.

The third column of Table IV lists the theoretical values $(\omega_K\tau_K)_T$, while the fourth column contains the $(\omega_K\tau_K)_{H2S}$

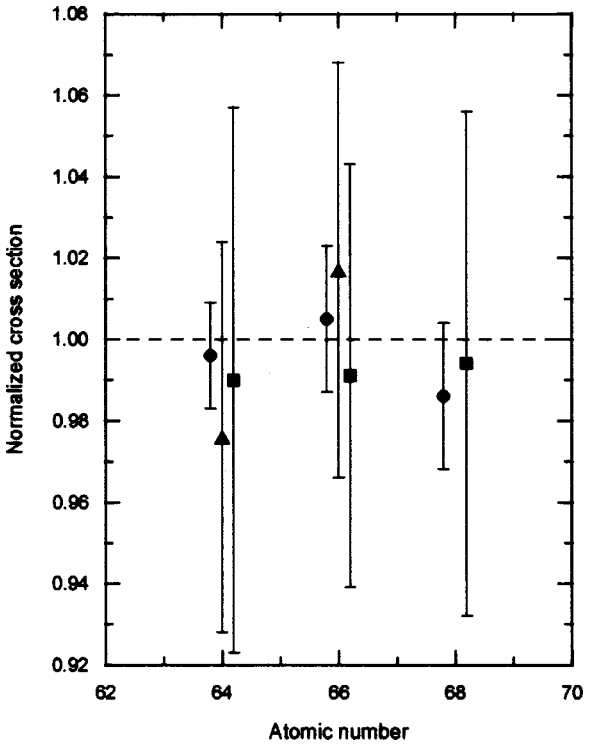

FIG. 2. Experimental K radiation emission photoelectric cross sections normalized to theoretical values (see text). Circles, present experiment; triangles, derived from the data of Balakrishna *et al.* [22]; squares, derived from the data of Ertuğrul *et al.* [23].

value obtained by the ^{66}Dy ω_K of Hubbell *et al.* [9]. Column five shows the $(\omega_K\tau_K)_F$ results of the present experiment, together with their absolute standard deviations. In columns six and seven the $(\omega_K\tau_K)_B$ and $(\omega_K\tau_K)_E$ values derived from the data of Balakrishna *et al.* [22] and Ertuğrul *et al.* [23] are given together with the uncertainties derived from those quoted by the authors.

The experimental $(\omega_K\tau_K)_F$, $(\omega_K\tau_K)_B$, and $(\omega_K\tau_K)_E$ values normalized to the theoretical $(\omega_K\tau_K)_T$ for atoms of Z equal to 64, 66, 68 stimulated by 59.54-keV photons are given in Fig. 2. The agreement between the present experimental results and the theoretical values is well within the quoted standard deviations. This corroborates the calculation procedures, at least in the region explored, even more so because the experimental uncertainties are rather small. Moreover, Table IV shows that the $(\omega_K\tau_K)_{H2S}$ ^{66}Dy value appears a little higher with respect to the present result, owing to the greater ω_K amount; in any case it falls within the 95% confidence interval of the experimental datum.

CONCLUSIONS

The present experimental measurements of K radiation emission cross sections of ^{64}Gd, ^{66}Dy, and ^{68}Er stimulated by 59.54-keV photons, i.e., an energy close to the K thresholds, have rather small uncertainties thanks to the use of thick target foils. They hence provide a useful reference for a global test of the theoretical models used in the K fluorescence yield calculations by Perkins *et al.* [3] and K photoelectric cross section evaluations by Scofield [16,36]. The agreement found is very good, and can be extended to other models giving highly similar results. Moreover, the values derived from the experiments carried out by Balakrishna *et al.* [22] and Ertuğrul *et al.* [23], with thin targets, agree with the present ones, even if their experimental approach gives greater uncertainties.

ACKNOWLEDGMENTS

The authors are grateful to Dr. J. H. Scofield and Dr. L. Kissel for their helpfulness in providing evaluations of photoelectric cross sections, and to Dr. J. H. Hubbell, who supplied the tabulations of atomic data. Special thanks are due to Dr. E. Luppi for her assistance in computing work, and to A. Magnani for his technical support. This experiment was supported by MURST (Rome), INFN (Rome), and the Emilia-Romagna Region (Bologna). One of us (B.S.) is especially obliged to ICTP (Trieste) for the grant that permitted him to participate in this experiment.

[1] M. H. Chen, B. Crasemann, and H. Mark, Phys. Rev. A **21**, 436 (1980).
[2] J. H. Scofield, Phys. Rev. A **9**, 1041 (1974).
[3] S. T. Perkins, D. E. Cullen, M. H. Chen, J. H. Hubbell, J. Rathkopf, and J. H. Scofield, Lawrence Livermore Laboratory Report No. UCRL 50400, Vol. 30, 1991 (unpublished).
[4] J. H. Scofield, Phys. Rev. **179**, 9 (1969).
[5] W. Bambynek, B. Crasemann, R. W. Fink, H. U. Freund, H. Mark, C. D. Swift, R. H. Price, and P. V. Rao, Rev. Mod. Phys. **44**, 716 (1972).
[6] M. O. Krause, J. Phys. Chem. Ref. Data **8**, 307 (1979).
[7] J. H. Hubbell, National Institute of Standards and Technology Report No. NISTIR 89-4144, 1989 (unpublished).
[8] W. Bambynek, in *X-84 Proceedings of X-Ray and Inner-Shell Processes in Atoms, Molecules and Solids, Leipzig, 1984*, edited by A. Meisel (Thomas Munzer, Langensalza, 1984), Paper P-1.
[9] J. H. Hubbell, P. N. Trehan, Nirmal Singh, B. Chand, D. Mehta, M. L. Garg, R. R. Garg, S. Singh, and S. Puri, J. Phys. Chem. Ref. Data **23**, 339 (1994).
[10] R. H. Pratt, A. Ron, and H. K. Tseng, Rev. Mod. Phys. **45**, 273 (1973).
[11] J. W. Cooper, in *Atomic Inner-Shell Processes*, edited by B. Crasemann (Academic, New York, 1975), Vol. I, pp. 159–199.
[12] J. H. Hubbell and W. Veigele, National Bureau of Standards Technical Note No. 901, 1976 (unpublished).
[13] A. F. Starace, in *Handbook der Physik*, edited by W. Mehlhorn (Springer-Verlag, Berlin, 1982), Vol. XXXI, pp. 1–121.
[14] E. Storm and H. I. Israel, Nucl. Data Tables **7**, 565 (1970).
[15] E. F. Plechaty, D. E. Cullen, and R. J. Howerton, Lawrence Livermore National Laboratory Report No. UCRL 50400, 1981 (unpublished).
[16] J. H. Scofield, Lawrence Livermore National Laboratory Report No. UCRL 51326, 1973 (unpublished).
[17] L. Kissel, R. H. Pratt, and S. C. Roy, Phys. Rev. A **22**, 1970 (1980).
[18] M. J. Berger and J. H. Hubbell, National Bureau of Standards Report No. NBSIR 87-3597, 1987 (unpublished).
[19] D. E. Cullen, J. H. Hubbell, and L. Kissel, Lawrence Livermore National Laboratory Report No. UCRL-LR-50400, Vol. 6, Rev. 5, 1998 (unpublished).
[20] C. T. Chantler, J. Phys. Chem. Ref. Data **24**, 71 (1995).
[21] L. Kissel, B. Zhou, S. C. Roy, S. K. Sen Gupta, and R. H. Pratt, Acta Crystallogr., Sect. A: Found. Crystallogr. **51**, 271 (1995).
[22] K. M. Balakrishna, N. G. Nayak, N. Lingappa, and K. Sidappa, J. Phys. B **27**, 715 (1994).
[23] M. Ertuğrul, Ö. Simsek, O. Doğan, and Ü. Turgut, J. Radioanal. Nucl. Chem. **213**, 37 (1996).
[24] E. Casnati, C. Baraldi, and A. Tartari, Phys. Rev. A **42**, 2627 (1990).
[25] E. Casnati, C. Baraldi, and A. Tartari, Phys. Rev. A **44**, 1699 (1991).
[26] C. M. Lederer and V. S. Shirley, *Tables of Isotopes*, 7th ed. (Wiley, New York, 1978).
[27] C. Baraldi, E. Casnati, A. Tartari, M. Andreis, and B. Singh, Phys. Rev. A **54**, 4947 (1996).
[28] E. Casnati, C. Baraldi, A. Tartari, and B. Singh, Appl. Radiat. Isot. **44**, 1155 (1993).

[29] Y. Namito, S. Ban, and H. Hirayama, Nucl. Instrum. Methods Phys. Res. A **349**, 489 (1994).
[30] S. Wagner, in *Ionizing Radiation Metrology*, edited by E. Casnati (Compositori, Bologna, 1977), pp. 409–417.
[31] J. H. Scofield, in *Atomic Inner-Shell Processes* (Ref. [11]), Vol. 1, pp. 265–292.
[32] M. R. Khan and M. Karimi, X-Ray Spectrom. **9**, 32 (1980).
[33] W. J. Veigele, At. Data **5**, 52 (1973).
[34] J. H. Hubbell, W. J. Veigele, E. A. Briggs, R. T. Brown, D. T. Cromer, and R. J. Howerton, J. Phys. Chem. Ref. Data **4**, 471 (1975); **6**, 615 (E) (1977).
[35] L. Kissel and P. M. Bergstrom, Jr., tabulations available from ftp://www-phys.llnl.gov/pub/rayleigh/SM
[36] J. H. Scofield (private communication).
[37] L. Kissel (private communication).